



Degradation of methyl orange through synergistic effect of Cu/Cu₂O nanoporous composite and ultrasonic wave

Huawei Jiang^{a,b}, Jie Li^a, Zhen Mu^a, Haoran Geng^{a,c,*}

^aSchool of Materials Science and Engineering, University of Jinan, No. 336, West Road of Nan Xinzhuang, Jinan 250022, P.R. China, Tel. +86 531 82765314; emails: jhwxin@163.com (H. Jiang), 2425738495@qq.com (J. Li), muzhen112@126.com (Z. Mu), mse_genghr@ujn.edu.cn (H. Geng)

^bYantai Lutong Precision Aluminium Industry Co., Ltd., Yantai 264006, P.R. China

^cShandong Provincial Key Laboratory of Preparation and Measurement of Building Materials, University of Jinan, No. 336, West Road of Nan Xinzhuang, Jinan 250022, P.R. China

Received 20 December 2013; Accepted 1 June 2014

ABSTRACT

The catalyst of nanoporous copper, covering a Cu₂O layer, was synthesized via the combination of dealloying of melt-spun Al₇₅Cu₂₅ (at.%) precursor alloy in acid solution with subsequent surface oxidation in air. The microstructure of the as-prepared catalyst has been characterized by X-ray diffraction and a field-emission scanning electron microscope. The results show that the as-prepared catalyst exhibits an open, bicontinuous interpenetrating ligament/channel structure, and is comprised of Cu and Cu₂O phases. Methyl orange (MO) was used as the model pollutant and the degradation experiments were carried out under dark conditions. The results of the experiment show that the Cu/Cu₂O nanoporous composite and the ultrasonic wave have the synergistic degradation effect for MO. And, the effect of pH value of MO solution, additive amounts of catalyst, initial concentrations of MO and inorganic ions on the degradation process has been investigated. The degradation mechanism of the as-prepared catalyst has also been discussed.

Keywords: Cu/Cu₂O; Ultrasonic wave; Methyl orange; Synergistic degradation

1. Introduction

Azo dyes constitute about a half of global dye-stuff production; the production and use of azo dyes result in environmental pollution due to the colour visibility and the toxicity of certain dyes [1], and about 15% of them are directly discharged into water without proper treatment [2]. A wide range of methods have been developed to treat dyes, including adsorption,

biodegradation, Fenton and photocatalytic degradation [3–5]. But the high cost, secondary pollution or low efficiency, etc. limit their development. However, due to cleanness and non-secondary pollution, the ultrasonic degradation has received increasing attention [6–8]. In the process of ultrasonic degradation, the sonoluminescence and hotspots caused by acoustic cavitation in a liquid can generate lights with a wide range of wavelengths and temperatures of around 5,000–10,000°C [9]. These conditions lead to the production of highly reactive radical species to attack and

*Corresponding author.

oxidize organic pollutants. However, the use of ultrasonic wave alone may not be suitable for all kinds of pollutants. To solve this problem, catalysts are added into the ultrasonic reaction system to reduce the activation energy [10], so that the reaction can be accelerated.

Studies have pointed out that with the presence of UV light or ultrasonic irradiation as the energy source, electron (e^-) of TiO_2 can be promoted from the valence band into the conduction band, leaving a hole (h^+) behind by furnishing energy matching or exceeding the band gap energy of the catalyst, and the holes can accelerate the dissociation of water molecules to form hydroxyl radical ($\cdot OH$), and then participate in the degradation of organic pollutants in water [11,12]. Thus, the presence of TiO_2 can significantly accelerate the generation of $\cdot OH$ as compared with that caused by the sonolysis of water molecule alone [13]. In addition, in order to improve the catalytic efficiency, modifications of TiO_2 have been explored to promote the separation of the electron-hole pairs during the catalytic reaction [14,15]. Xue et al. reported that combining TiO_2 with some narrow band gap semiconductors, for instance CdS (2.41 eV), the response of TiO_2 can be extended to the visible light region and the photocatalytic performance can be improved [16]. Recently, a novel Cu/ Cu_2O composite has attracted the attention of people. This is because compared with TiO_2 (3.0–3.2 eV), Cu_2O has a narrower band gap (2.0–2.2 eV) [17,18], so e^- of Cu_2O in valence band is easier to be excited to conduction band, resulting in a hole. In addition, the heterojunction of Cu and Cu_2O can enhance the catalytic property of Cu_2O -based semiconductors, because the existence of Cu can promptly transfer electrons, avoiding the recombination of electron-hole pairs [19,20].

In this work, we aimed at the design and fabrication of a novel Cu/ Cu_2O nanoporous composite catalyst through surface oxidation nanoporous copper (NPC), obtained by dealloying and then studied the degradation of methyl orange (MO) through joint action of Cu/ Cu_2O nanoporous composite and ultrasonic wave. NPC was firstly prepared by dealloying the Al–Cu precursor in acidic media. Subsequently, surface oxidation resulted in the formation of Cu/ Cu_2O nanoporous composite. In degradation experiments, MO was used as the model pollutant because it is widely used in textile, printing, paper manufacturing, pharmaceutical and food industries [21]. The effect of pH value, additive amounts of catalyst, initial concentrations of MO and inorganic anions on the catalytic activity has been investigated under the condition of ultrasonic away from light.

2. Experimental

2.1. Preparation and characterization of Cu/ Cu_2O nanoporous composite

Al–Cu alloy with nominal compositions of $Al_{75}Cu_{25}$ (at.%) was prepared from pure Al (99.9 wt.%), and pure Cu (99.9 wt.%). Voltaic arc heating was employed to melt the charges in a copper crucible under an argon atmosphere, and then the melt was cooled down into ingots *in situ*. By use of a single-roller melt-spinning apparatus, the alloy ingots were remelted in a quartz tube by high-frequency induction heating and then melt-spun onto a copper roller (diameter, 0.22 m) at a roller speed of ~2000 rpm in a controlled argon atmosphere.

The dealloying of the melt-spun ribbons was performed in a 5 wt.% HCl solution at room temperature. After dealloying, the samples were rinsed with distilled water and dehydrated alcohol. Finally, the as-dealloyed samples were kept in a vacuum oven for drying and preservation. The catalyst was obtained by the following surface oxidation in air at ambient temperature for three days. The phase constitution of the as-prepared catalyst was characterized by X-ray diffraction (XRD, Rigaku D/max-rB) with Cu/ $K\alpha$ radiation. The field emission scanning electron microscope (FE-SEM, FEI QUANTA FEG 250) with an energy dispersive X-ray (EDS) analyzer was employed to study the morphology and nanoporous structure of the as-prepared catalyst.

2.2. The degradation experiment of MO

To study the synergistic effect of Cu/ Cu_2O nanoporous composite and ultrasonic wave, the degradation experiments were carried out under dark conditions. The ultrasonic frequency is 40 kHz, and the ultrasonic power is 100 W. The pH of MO solution was adjusted with hydrochloric acid and potassium hydroxide solutions. The pH was measured with a pH meter (Model PHS-3D, China). Cu/ Cu_2O nanoporous composite was dispersed in 50 mL beakers containing 50 mL MO solution. A small amount of MO solution (4 mL) was extracted at certain intervals and the absorbance of MO solution was monitored by a visible spectrophotometer (Model 722, China) at 463 nm, which is the maximum absorbance wavelength of MO solution. The degradation efficiency of the MO solution was calculated with the following equation:

$$\eta = (A_0 - A)/A_0 \times 100\% \quad (1)$$

where A_0 is the original absorbance of MO solution at its maximum absorbance wavelength and A is the absorbance of MO solution at the same wavelength after different degradation durations.

3. Results and discussion

3.1. Fabrication and characterization of catalyst

Fig. 1 shows the XRD pattern of the as-prepared catalyst. There are three major diffraction peaks ($2\theta = 43.3, 50.4$ and 74.1°) in the XRD pattern, corresponding to the (111), (200) and (220) reflections of a face-centred cubic (f.c.c.) Cu (PDF # 04-0836), respectively. In addition, there are two minor diffraction peaks ($2\theta = 36.5$ and 61.5°) which is indexed to Cu_2O (PDF # 65-3288), corresponding to the (111) and (220) reflections, respectively. It should be noted that the diffraction peaks of Cu_2O at 42.4 and 73.7° may overlap with the (111) and (220) reflections of Cu, respectively, and the diffraction peaks of Cu_2O at 29.6° does not occur. Therefore, the as-obtained catalyst is composed of Cu and Cu_2O phases and Cu is dominant according to the relative intensities of both phases (Fig. 1).

The crystallite size calculation can be made using Debye-Scherrer equation:

$$L = 0.89 \lambda / (\beta \cos \theta) \quad (2)$$

where L is the crystalline size (nm), λ is X-ray wavelength (1.5406 \AA), β is full width at half maximum measured in radians, θ is the Bragg diffraction

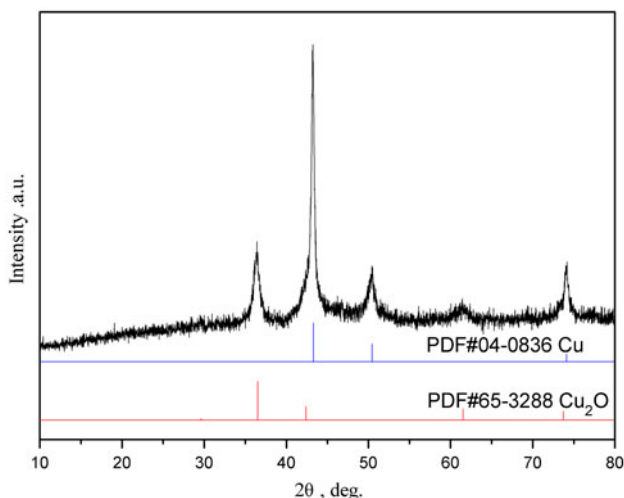


Fig. 1. XRD pattern of as-prepared catalyst obtained through dealloying of melt-spun Al75Cu25 alloy ribbons and subsequent surface oxidation in air.

angle ($^\circ$). Here, the as-prepared catalyst is taken as a polycrystalline composed of Cu and Cu_2O , Cu is inside and Cu_2O is outside. The average crystalline size of Cu and Cu_2O is figured out from the Debye-Scherrer formula. The result shows that the average crystalline size of Cu and Cu_2O is about 26 and 17.5 nm, respectively. In addition, it should be noted that Cu_2O particles with a diameter less than 25 nm are more stable than CuO phase [22,23], that is to say, the Cu_2O in as-prepared catalyst cannot be further oxidized to form CuO and is stable.

Fig. 2 shows the morphology and nanoporous structure of the as-prepared catalyst. Fig. 2(a) shows the morphology of one as-prepared catalyst, ribbon, and the thickness of the ribbon is about $20 \mu\text{m}$. As shown in Fig. 2(b), the bicontinuous interpenetrating ligament/channel structure can be clearly seen. The size of channels is about 30–60 nm and that of ligaments is about 40–70 nm. The EDS result demonstrates that the as-prepared catalyst is mainly composed of Cu, O and a minor amount of residual Al. A typical EDS spectrum is presented in Fig. 2(c).

3.2. Synergistic effect of Cu/ Cu_2O nanoporous composite and ultrasonic wave

In order to make the synergistic effect of Cu/ Cu_2O nanoporous composite and ultrasonic wave shown fully, a series of affecting factors have been studied in this paper. Firstly, the effect of pH value of MO solution on the degradation process was studied. The pH value of MO solution has great influence on the degradation process. Fig. 3 shows the influence of pH value on degradation efficiency when the reaction time is 50 min, the concentration of MO solution is 20 mg/L and the additive amount of catalyst is 0.4 g/L. From Fig. 3, it can be seen that the degradation efficiency under different pH values shows the following rules: $\text{pH} (7.09) > \text{pH} (5.11) > \text{pH} (9.07) > \text{pH} (3.13) > \text{pH} (1.92) > \text{pH} (11.05) > \text{pH} (12.26)$. The degradation efficiency of MO solution among pH 3.13–9.07 is all more than 94% after 50 min, especially, the degradation efficiency reaches 100% at pH 7.09. Under strong acid and strong alkali environment, the degradation efficiency of MO solution is very low: the degradation efficiency is about 24, 3.7 and 2.2% at pH 1.92, 11.05 and 12.26, respectively.

There are two main reasons for the strong influence of pH value. On one hand, the pH value of the solution can affect the amount of adsorbed species by changing the surface charge [24]. In acidic solution, surface hydroxyl group of Cu/ Cu_2O nanoporous composite is acidic to a certain degree and they exist in the form of $-\text{OH}$. While in alkaline solution, the

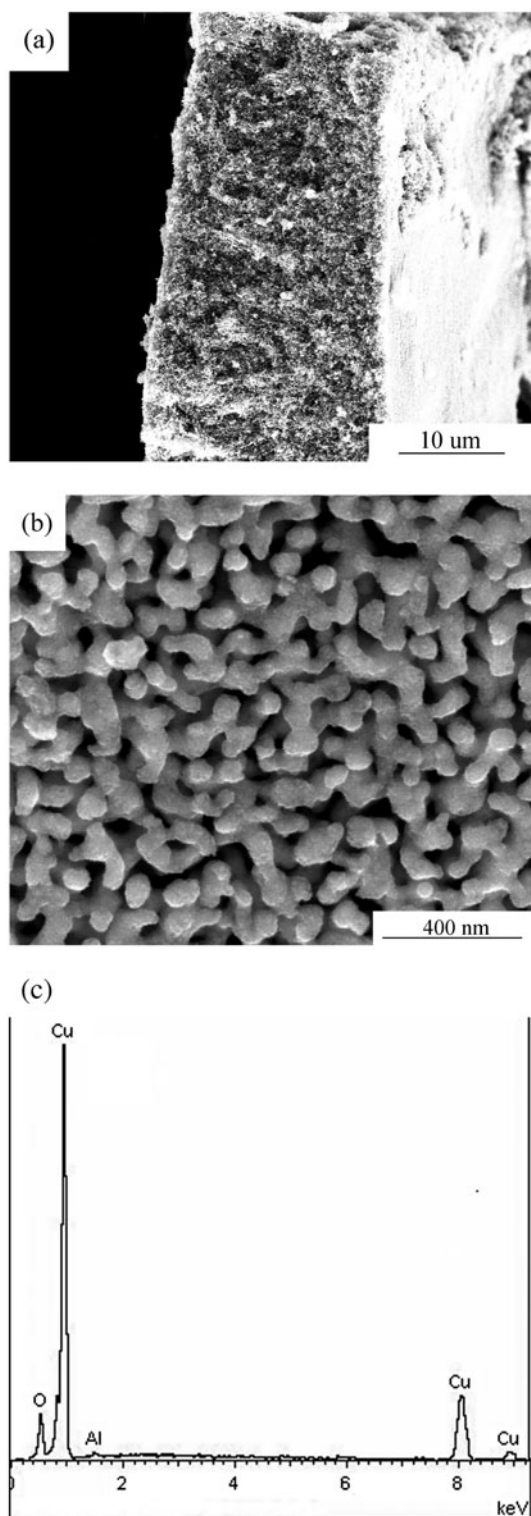


Fig. 2. SEM images showing (a) as-prepared catalyst ribbon, (b) nanoporous structure of as-prepared catalyst and (c) A typical EDX spectrum.

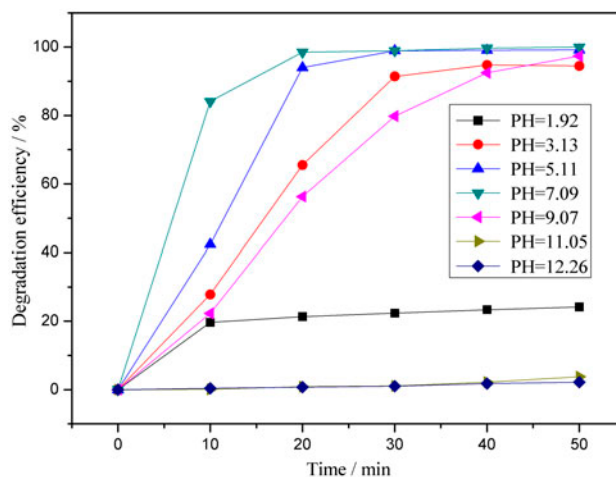


Fig. 3. Influence of pH value on degradation efficiency of MO.

surface hydroxyl group exists in the form of $-O^-$. This change would affect the adsorption of MO onto Cu/Cu₂O nanoporous composite. On the other hand, the pH value of the solution has an impact on the stability of Cu₂O. Feng et al. found that monoclinic CuO film can form above the pH value of 12, and the film thickness can increase quickly with greater alkalinity [25]. In addition, the Cu₂O oxide film tends to dissolve in acidic solution, while the film thickness decreases rapidly with pH decreasing below 4, so it can be supposed that the Cu₂O oxide film covering on NPC may have been changed into CuO at pH 11.05 in this experiment. When the pH value is higher than 11.05, the MO almost cannot be degraded; while, when the pH value is lower than 3.13, the Cu₂O oxide film dissolves gradually. Until the pH value reaches 1.92, there is still a little residual Cu₂O covering on NPC which can degrade a small amount of MO.

The studies on the effect of additive amounts of catalyst on the degradation process were carried out at pH 7.09. Fig. 4 shows that the degradation efficiency of MO solution under different additive amounts of Cu/Cu₂O nanoporous composite catalyst. Without catalysts, ultrasonic degradation efficiency of MO solution is only 6.5% after 50 min. With the increase in catalyst, degradation efficiency increases gradually and then decreases. This is because the number of $\cdot OH$ increases with the increase in additive amounts of catalyst, leading to a higher degradation efficiency. But when the amount of the catalyst is more, the catalyst produces a mutual shielding effect, reducing the utilization of ultrasonic wave and thus,

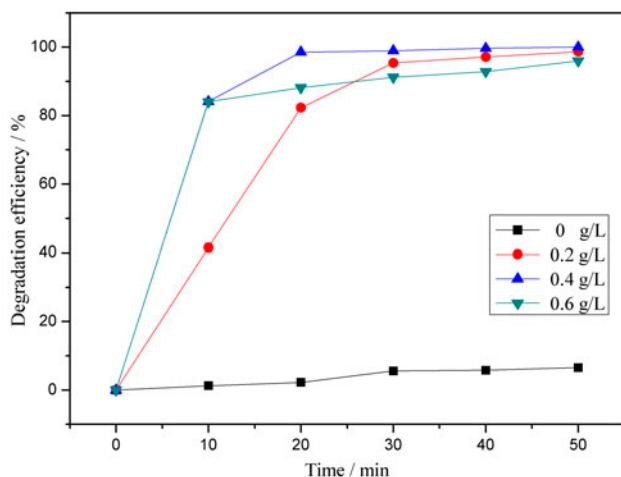


Fig. 4. Influence of additive amounts of catalyst on degradation efficiency of MO.

making a decrease in degradation efficiency. We can see from Fig. 4, after 50 min ultrasonic degradation, the degradation efficiency of MO solution is 98.6, 100 and 95.9% with 0.2, 0.4 and 0.6 g/L catalyst respectively.

The effect of initial concentration of MO solution on the degradation process was studied by varying the initial concentration of MO solution from 10 to 40 mg/L. The additive amount of catalyst is 0.4 g/L and the pH value is 7.09. Fig. 5 shows the relationship between the degradation efficiency of MO solution and the initial concentration of MO. It can be seen, from Fig. 5, that the degradation rate of different initial concentrations of MO solution is different in different time periods. Therefore, different concentrations of curves produce crosses. Although the degradation rate of different

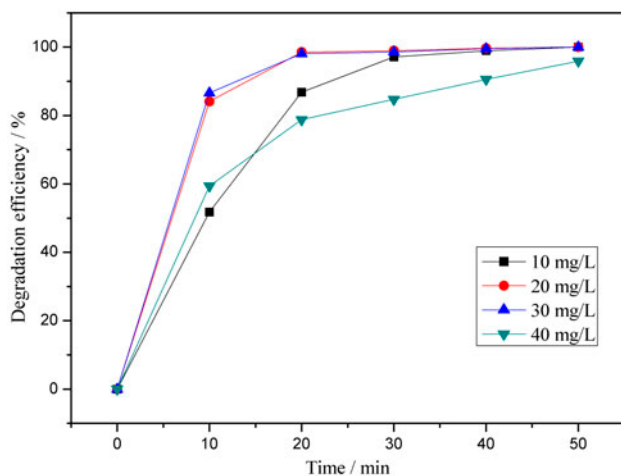


Fig. 5. Influence of initial concentrations of MO solution on degradation efficiency of MO.

initial concentrations of MO solution changed continuously in the degradation process, the degradation efficiency of 10, 20 and 30 mg/L MO solution all reaches to 100% after 50 min, while the degradation efficiency of 40 mg/L MO solution is close to 96%, and after a long time, the 40 mg/L MO solution can also be degraded completely.

Under normal circumstances, the degradation rate will slow down with the increase in initial concentration of dye gradually, this is because the adsorbed amount of dye molecules on the surface of the catalyst would increase with the increase in dye, causing the reduction of active site producing $\cdot\text{OH}$, and then resulting in the decrease in dye degradation efficiency. Of course, there are exceptions, this is mainly because the degradation rate also depends on the chance of dye molecules in contact with $\cdot\text{OH}$ [26].

As we all know, some dye wastewater often contains some inorganic anions (such as NO_3^- , SO_4^{2-} , Cl^- , etc.), which can produce effects on the degradation of dye. In this paper, 0.01 mol/L NaCl, NaNO_2 , NaNO_3 , Na_2SO_3 and Na_2SO_4 solution were added into 20 mg/L MO solution and the additive amount of catalyst was 0.4 g/L and the pH value was 7.09. Avoiding light for 50 min, the ultrasonic degradation efficiency of MO solution is shown in Fig. 6; here the influence of Na^+ is ignored [27]. We found that the addition of Cl^- etc. inorganic anions inhibit the degradation of MO. But the degradation efficiency of MO solution containing Cl^- , NO_2^- and NO_3^- can still reach more than 92% in 50 min, while the degradation efficiency of MO solution containing SO_3^{2-} , SO_4^{2-} is 72.3 and 52.9%, respectively.

The addition of inorganic anions played two roles in the degradation of MO [28]. The first one is that,

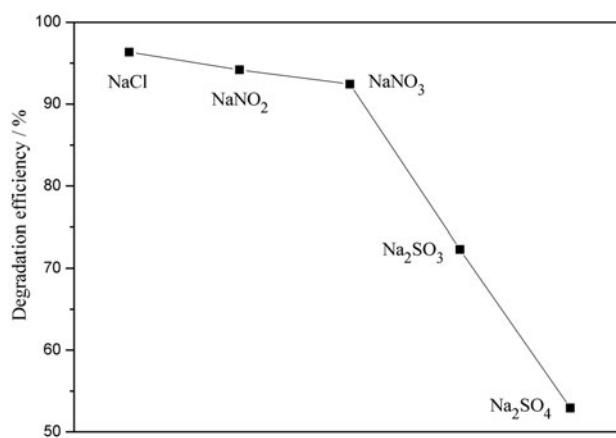
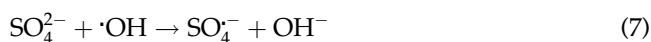
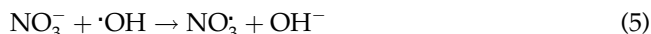


Fig. 6. Influence of inorganic anions on degradation efficiency of MO.

inorganic anions affect the ultrasonic degradation of MO by changing the surface charge of catalyst, resulting in a change of distribution of MO molecules between the solution and catalyst surface. Another is that, the adsorbed inorganic anions react with $\cdot\text{OH}$, as shown in Eqs. (3)–(7):



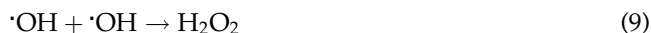
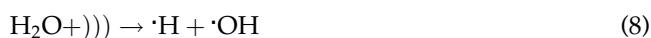
Cl^\cdot , NO_2^\cdot , NO_3^\cdot , SO_3^\cdot and SO_4^\cdot are less reactive than $\cdot\text{OH}$, therefore, the inorganic anions hinder the degradation efficiency of MO solution.

In order to prove that the Cu/Cu₂O nanoporous composite and the ultrasonic wave have a synergistic effect on the degradation of MO, the experiment without ultrasonic wave was carried out under dark conditions. The value of pH is 7.09, the additive amount of catalyst is 0.4 g/L and the initial concentration of MO is 20 mg/L. From Fig. 7, it can be found that the degradation efficiency of MO solution is close to 12% (curve 2). However, it is well known that the photocatalysts have no activity for the degradation of dyes if without energy light. Here, it can be explained that the adsorption of nanoporous structure makes part of MO to adsorb on the surface of the catalyst and

causes the decrease in the original concentration of MO, eventually resulting in the decrease in the absorbance of MO. Compared with the experimental results under the effect of ultrasonic wave, it is higher than the degradation efficiency obtained under the effect of ultrasonic wave alone (curve 3) and is lower nearly 90% than that obtained under the synergy of Cu/Cu₂O nanoporous composite and ultrasonic wave (curve 1).

3.3. Possible sonocatalytic mechanism of Cu/Cu₂O nanoporous composite

The application of ultrasonic wave in water with a frequency range between 18 and 100 MHz can result the phenomenon of acoustic cavitation [11,12,29]. Hydrogen radical ($\cdot\text{H}$), $\cdot\text{OH}$ and hydrogen peroxide (H_2O_2) can be produced in this process (Eqs. (8) and (9)):



Here, the sonocatalytic mechanism of MO on the surface of Cu/Cu₂O nanoporous composite can be explained by two relatively mature mechanisms. One explanation is that, the ultrasonic cavitation generates high energy light. Light can produce $\cdot\text{OH}$ with high oxidation-activity. This makes sonocatalysis similar to photocatalysis, and the mechanism of degradation is depicted in Fig. 8(a). Under the high-energy light, Cu₂O semiconductor oxide can be excited to produce electrons and holes. The generated electrons and holes can initiate a series of degradation reactions. Holes in the valence band can oxidize hydroxyl ions (OH^-) adsorbed on the surface of the catalyst to yield $\cdot\text{OH}$ which plays an important role in degradation [30,31]. Electrons can transfer from Cu₂O to Cu through the crystal interphase, resulting in the complete separation of electrons and holes which plays an important role in improving catalytic activity. In addition, electrons conducted by Cu can be captured by adsorbed oxygen molecules (O_2), leading to the generation of super oxide radical ions (O_2^\cdot) [32]. O_2^\cdot can further interact with H_2O_2 resulting in OH^- and $\cdot\text{OH}$, and then promote the degradation process of MO [33]. Finally, MO can be oxidized into intermediates. Another explanation is that, heterogeneous Cu₂O catalyst absorbs thermal energy produced by ultrasonic wave, causing oxygen atoms to escape the lattice and then generate holes. Holes can oxidize OH^- adsorbed on the surface of the catalyst to yield $\cdot\text{OH}$. Finally, MO can be oxidized into intermediates by $\cdot\text{OH}$ (Fig. 8(b)).

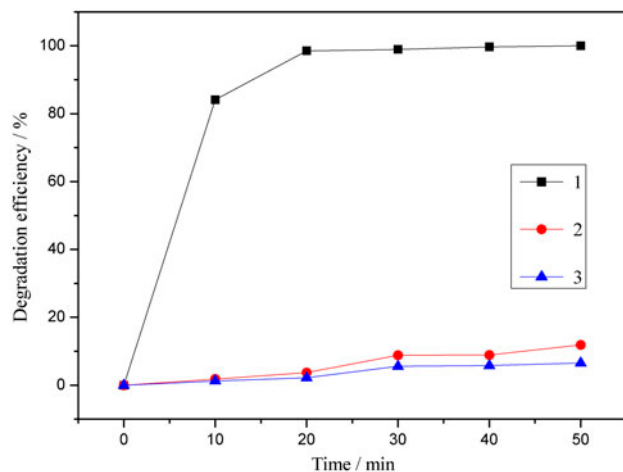


Fig. 7. Degradation efficiency of MO (1: ultrasonic wave + Cu/Cu₂O nanoporous composite; 2: Cu/Cu₂O nanoporous composite; 3: ultrasonic wave).

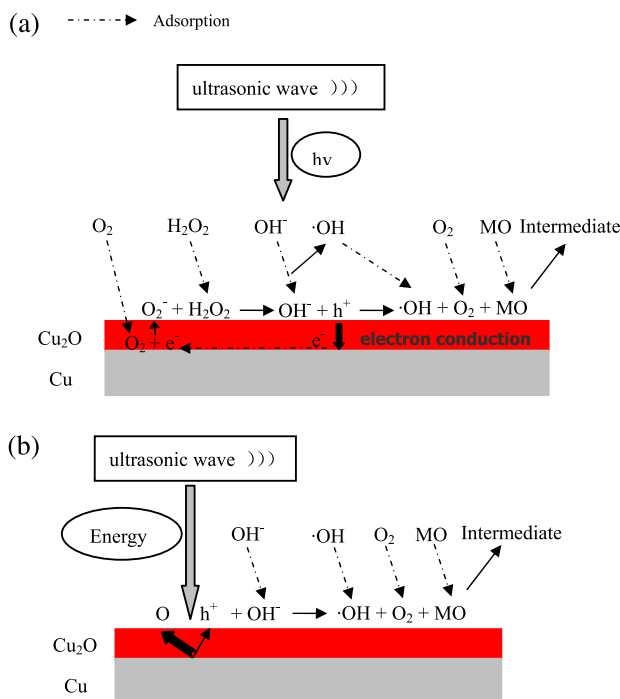


Fig. 8. Schematic diagrams for possible sonocatalytic mechanism of Cu/Cu₂O nanoporous composite.

4. Conclusions

The Cu/Cu₂O nanoporous composite catalyst was prepared through dealloying of the melt-spun Al₇₅Cu₂₅ ribbons in the HCl solution and subsequent surface oxidation in air. This catalyst shows superior catalytic activity towards the degradation of MO under the condition of ultrasonic and without light. Experimental results show that under the condition of strong acid and alkaline, the Cu/Cu₂O nanoporous composite catalyst can hardly degrade MO, which is caused by the dissolution of Cu₂O and the generation of CuO. Moreover, the additive amounts of catalyst, the initial concentrations of MO and inorganic anions have a significant effect on the degradation process and the catalytic activity. The best value for the additive amounts of catalyst and the initial concentration of MO is 0.4 g/L and 20 mg/L, respectively, and the addition of inorganic anions inhibits the degradation of MO. Under the synergistic effect of Cu/Cu₂O nanoporous composite and ultrasonic wave, MO can be degraded rapidly.

Acknowledgements

The authors would like to acknowledge the Natural Science Foundation of China (51271087) and the Natural Science Foundation of Shandong Province (ZR2010ZM071) with this work.

References

- [1] J. Hong, H. Emori, M. Otaki, Photodecolorization of azo dyes by extracellular metabolites under fluorescent light and influence of operational parameters, *J. Biosci. Bioeng.* 100 (2005) 192–196.
- [2] H. Park, W. Choi, Visible light and Fe(III)-mediated degradation of Acid Orange 7 in the absence of H₂O₂, *J. Photochem. Photobiol., A* 159 (2003) 241–247.
- [3] G. Annadurai, R. Juang, D. Lee, Use of cellulose-based wastes for adsorption of dyes from aqueous solutions, *J. Hazard. Mater.* 92 (2002) 263–274.
- [4] I.T. Peternel, N. Koprivanac, A.M.L. Božić, H.M. Kušić, Comparative study of UV/TiO₂, UV/ZnO and photo-Fenton processes for the organic reactive dye degradation in aqueous solution, *J. Hazard. Mater.* 148 (2007) 477–484.
- [5] E. Bae, W. Choi, Highly enhanced photoreductive degradation of perchlorinated compounds on dye-sensitized metal/TiO₂ under visible light, *Environ. Sci. Technol.* 37 (2003) 147–152.
- [6] E. Psillakis, G. Goula, N. Kalogerakis, D. Mantzavinos, Degradation of polycyclic aromatic hydrocarbons in aqueous solutions by ultrasonic irradiation, *J. Hazard. Mater.* 108 (2004) 95–102.
- [7] G. Tezcanli-Guyer, N.H. Ince, Degradation and toxicity reduction of textile dyestuff by ultrasound, *Ultrason. Sonochem.* 10 (2003) 235–240.
- [8] M. Inoue, F. Okada, A. Sakurai, M. Sakakibara, A new development of dyestuffs degradation system using ultrasound, *Ultrason. Sonochem.* 13 (2006) 313–320.
- [9] J. Wang, Y. Guo, B. Liu, X. Jin, L. Liu, R. Xu, Y. Kong, B. Wang, Detection and analysis of reactive oxygen species (ROS) generated by nano-sized TiO₂ powder under ultrasonic irradiation and application in sonocatalytic degradation of organic dyes, *Ultrason. Sonochem.* 18 (2011) 177–183.
- [10] L. Song, C. Chen, S. Zhang, Sonocatalytic performance of Tb₇O₁₂/TiO₂ composite under ultrasonic irradiation, *Ultrason. Sonochem.* 18 (2011) 713–717.
- [11] J. Wang, Z.J. Pan, Z.H. Zhang, X.D. Zhang, F.Y. Wen, T. Ma, Y.F. Jiang, L. Wang, L. Xu, P.L. Kang, Sonocatalytic degradation of methyl parathion in the presence of nanometer and ordinary anatase titanium dioxide catalysts and comparison of their sonocatalytic abilities, *Ultrason. Sonochem.* 13 (2006) 493–500.
- [12] M. Abbasi, N.R. Asl, Sonochemical degradation of basic blue 41 dye assisted by nanoTiO₂ and H₂O₂, *J. Hazard. Mater.* 153 (2008) 942–947.
- [13] A.Z. Abdullah, P.Y. Ling, Heat treatment effects on the characteristics and sonocatalytic performance of TiO₂ in the degradation of organic dyes in aqueous solution, *J. Hazard. Mater.* 173 (2010) 159–167.
- [14] G.D. Yang, Z.F. Yan, T.C. Xiao, B.L. Yang, Low-temperature synthesis of alkalis doped TiO₂ photocatalysts and their photocatalytic performance for degradation of methyl orange, *J. Alloys Compd.* 580 (2013) 15–22.
- [15] G.D. Yang, T. Wang, B.L. Yang, Z.F. Yan, S.J. Ding, T.C. Xiao, Enhanced visible-light activity of F-N codoped TiO₂ nanocrystals via nonmetal impurity, Ti³⁺ ions and oxygen vacancies, *Appl. Surf. Sci.* 287 (2013) 135–142.

- [16] C. Xue, T. Wang, G.D. Yang, B.L. Yang, S.J. Ding, A facile strategy for the synthesis of hierarchical TiO₂/CdS hollow sphere heterostructures with excellent visible light activity, *J. Mater. Chem. A* 2 (2014) 7674–7679.
- [17] I. Grozdanov, Electroless chemical deposition technique for Cu₂O thin films, *Mater. Lett.* 19 (1994) 281–285.
- [18] D. Jiang, Y. Xu, D. Wu, Y.H. Sun, Visible-light responsive dye-modified TiO₂ photocatalyst, *J. Solid State Chem.* 181 (2008) 593–602.
- [19] Y. Tang, Z. Chen, Z. Jia, L. Zhang, J. Li, Electrodeposition and characterization of nanocrystalline cuprous oxide thin films on TiO₂ films, *Mater. Lett.* 59 (2005) 434–438.
- [20] B. Zhou, Z. Liu, H. Wang, Y. Yang, W. Su, Experimental study on photocatalytic activity of Cu₂O/Cu nanocomposites under visible light, *Catal. Lett.* 132 (2009) 75–80.
- [21] S.C. Rastogi, V.J. Barwick, S.V. Carter, Identification of organic colourants in cosmetics by HPLC-diode array detection, *Chromatographia* 45 (1997) 215–228.
- [22] V.R. Palkar, P. Ayyub, S. Chattopadhyay, M. Multani, Size-induced structural transitions in the Cu-O and Ce-O systems, *Phys. Rev. B: Condens. Matter* 53 (1996) 2167–2170.
- [23] S. Ram, C. Mitra, Formation of stable Cu₂O nanocrystals in a new orthorhombic crystal structure, *Mater. Sci. Eng., A* 304–306 (2001) 805–809.
- [24] J.L. Zhao, X.X. Wang, L.B. Zhang, X.R. Hou, Y. Li, C.C. Tang, Degradation of methyl orange through synergistic effect of zirconia nanotubes and ultrasonic wave, *J. Hazard. Mater.* 188 (2011) 231–234.
- [25] Y. Feng, K.S. Siow, W.K. Teo, K.L. Tan, A.K. Hsieh, Corrosion mechanisms and products of copper in aqueous solutions at various pH values, *Corrosion* 53 (1997) 389–398.
- [26] C.Z. Jiang, H.D. Su, X.D. Lu, Photodegradation of methylene blue with mixing nanocrystal TiO₂ films, *Environ. Sci. Technol.* 31 (2008) 26–29.
- [27] M. Abdullah, G.K.C. Low, R.W. Matthews, Effects of common inorganic anions on rates of photocatalytic oxidation of organic carbon over illuminated titanium dioxide, *J. Phys. Chem.* 94 (1990) 6820–6825.
- [28] C. Hu, J.C. Yu, Z. Hao, P.K. Wong, Effects of acidity and inorganic ions on the photocatalytic degradation of different azo dyes, *Appl. Catal., B* 46 (2003) 35–47.
- [29] N.H. Ince, G.T. Guyer, Impacts of pH and molecular structure on ultrasonic degradation of azo dyes, *Ultrasonics* 42 (2004) 591–596.
- [30] M.M. Tauber, G.M. Gubitz, A. Rehorek, Degradation of azo dyes by oxidative processes-laccase and ultrasound treatment, *Bioresour. Technol.* 99 (2008) 4213–4220.
- [31] Z. Zheng, B. Huang, Z. Wang, M. Guo, X. Qin, X. Zhang, P. Wang, Y. Dai, Crystal faces of Cu₂O and their stabilities in photocatalytic reactions, *J. Phys. Chem. C* 113 (2009) 14448–14453.
- [32] A.P.L. Batista, H.W.P. Carvalho, G.H.P. Luz, P.F.Q. Martins, M. Goncalves, L.C.A. Oliveira, Preparation of CuO/SiO₂ and photocatalytic activity degradation of methylene blue, *Environ. Chem. Lett.* 8 (2010) 63–67.
- [33] L. Huang, F. Peng, H. Yu, H. Wang, Preparation of cuprous oxides with different sizes and their behaviors of adsorption, visible-light driven photocatalysis and photocorrosion, *Solid State Sci.* 11 (2009) 129–138.